Field Trials of a Prototype Lunar Rover under Multi-Sensor Safeguarded Teleoperation Control

E. Krotkov, M. Hebert, L. Henriksen, P. Levin, M. Maimone, R. Simmons, and J. Teza

Robotics Institute, School of Computer Science
Carnegie Mellon University, Pittsburgh, PA 15213

Abstract — This paper presents the results of field trials of a prototype lunar rover traveling over natural terrain under safeguarded teleoperation control. Both the rover and the safeguarding approach have been used in previous work. The original contributions of this paper are the development and integration of a laser sensing system, and extensive field testing of the overall system. The laser system, which complements an existing stereo vision system, is based on a line-scanning laser ranger viewing the area 1 meter in front of the rover. The laser system has demonstrated excellent performance: zero misses and few false alarms operating at 4 Hz. The overall safeguarding system guided the rover 43 km over lunar analogue terrain with 0.8 failures per kilometer.

1 Introduction

The hazard detection system described in this paper has been developed under CMU's Lunar Rover Initiative, whose goal is to develop and demonstrate techniques enabling planetary rover missions. The initiative has targeted a mission to land two rovers on the surface of the Moon, where they will navigate semi-autonomously for 1,000 km, visiting historic sites and places of geological interest (Krotkov 1994).

For such a mission, a spectrum of navigation modes are applicable. At one end of the spectrum lies pure teleoperation. Although this is feasible, as the Soviets showed in the 1960s with the Lunokhod program, the time delay proves troublesome and contributes to significant stress and fatigue for operators. At the other end of the spectrum lies pure autonomy. Although research in autonomous vehicles has progressed dramatically, it has not yet produced techniques for safe, reliable operation of rovers using limited computing and sensing resources.

Our approach, called ***safeguarded teleoperation,*** occupies a position in the center of the spectrum. In this approach, the user specifies high-level goals such as desired direction of travel, and the vehicle autonomously decides how to execute the command in a way that optimizes a performance criterion. The principal virtue of the approach is to enable safe and reliable operation, maintaining system integrity by avoiding environmental hazards and faulty uplink commands of the type that crippled the Phobos lander. The safeguarded teleoperation approach has been described in detail in several predecessor papers (Krotkov 1995, Simmons 1996).

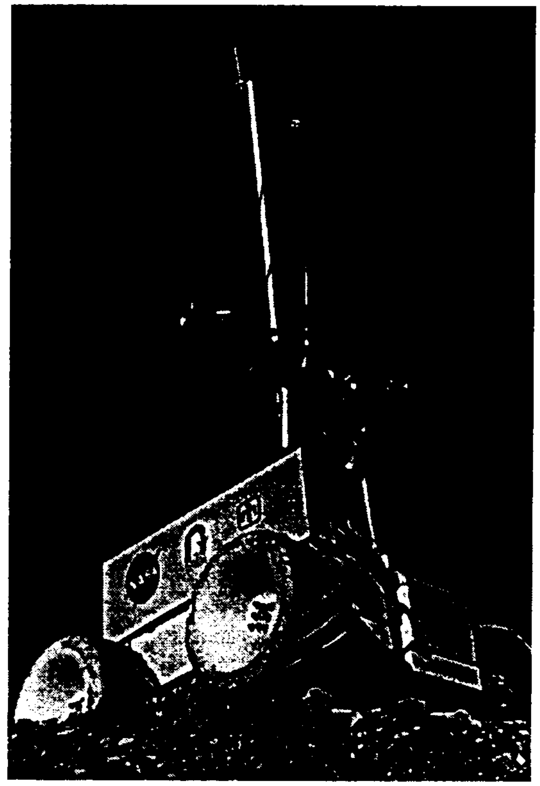

Figure 1. Ratler

In earlier work, we developed a stereo vision system (Krotkov 1995) to provide the data necessary to determine the level of threat posed by a surface in front of the rover, and tested it on the Ratler rover (Figure 1) (Purvis & Klarer, 1992). The implemented four-camera system features an 80 degree field of view, and processes terrain data 4 to 8 meters in front of the vehicle at approximately 1 Hz, with a typical ground resolution of 8 cm. A local obstacle avoidance planner uses the stereo data to determine a path for the rover which poses the least threat to the integrity of the vehicle. Experience with the vision system shows that it keeps the rover out of hazardous situations most of the time, but there are features it has problems detecting. For example, stereo vision often cannot detect craters, instead reporting them as unknown areas; this is not a limitation of the stereo algorithm, but of the stereo field of view, which causes the proximal crater region to be occluded by the crater rim. In addition, the large look-ahead distance and the resulting low resolution means that small obstacles may be missed.

To complement the stereo system and provide a redundant sensor, we have developed a laser-based hazard detection system. The implemented system provides data with ground resolution better than 1 cm at rates in excess of 4 Hz. We point the laser at the area some 75 to 125 cm in front of the vehicle, so that it cap detect the troublesome depressions like craters. **As** a consequence, when the laser system detects an obstacle, there is insufficient time to maneuver, and instead an emergency stop command must be issued and the obstacle avoidance planner notified. In addition to responding to terrain depressions, the laser system contributes to the overall safety by sensing areas not covered by stereo vision when performing a point turn, and by detecting small objects missed due to the coarse resolution of the vision system.

The combination of a stereo vision system and a laser line scanner possesses several advantages over a single 2D laser ranger (Kelly 1995). First, it would be difficult to manufacture a 2D laser scanner that has both the wide field of view laterally and horizontally and at the same time maintaining an update rate high enough to react to obstacles just in front of the rover. The combination of the slower long-range stereo vision system and the faster short-range laser line scanner provides data at rates necessary for each range. Second, a 2D scanner is mechanically more complex than the combination of the cameras and a simple line scanner, making the overall system potentially more robust. Since the lunar mission has a time span of years, longevity becomes an important issue. Third, splitting the sensing task into a vision and a laser part builds in a level of redundancy enabling mission continuation despite either sensor becoming unavailable.

The first primary contribution reported in this paper is in integrating the laser sensing system into the safeguarded teleoperation framework established in previous work. Figure 2 illustrates the implemented system, which differs from our previous systems in the addition of the laser sensing system, and in moving all safeguarding processing on-board the rover. The second primary contribution reported in this paper is in conducting extensive tests of the overall system, in which it drove the rover 43 km over lunar analogue terrain under realistic conditions.

This paper is organized as follows. In the next section it presents the laser sensing system, including the sensor and the approach to hazard detection. In Section 3 it describes the safeguarded teleoperation experiments, and summarizes their results in Section 4. The paper concludes with a discussion of concrete ideas for future work.

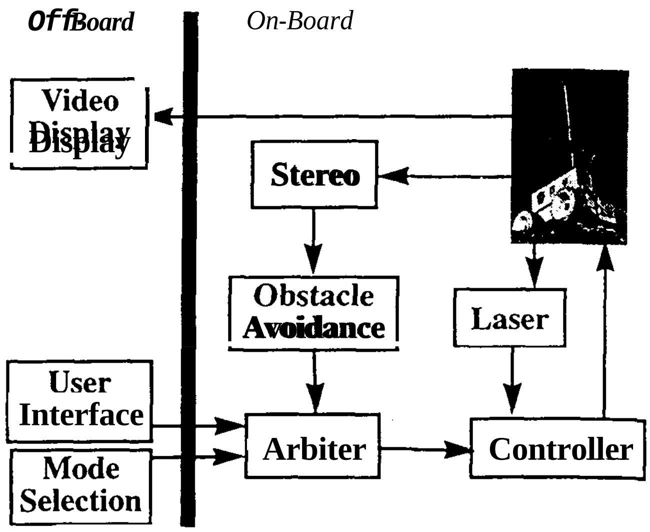

Figure 2. Safeguarded teleoperation system architecture

2 Laser Sensing System

A number of researchers have developed algorithms and systems with 1D laser scanners. The longer-range sensors, such as the laser systems on Adam (Chatila 1996) and Dante (Krotkov 1994), have typically been used for mapping or reconstructing the environment, and then performing hazard detection. Experience has shown that this approach is relatively slow and somewhat fragile. The shorter-range sensors, such as the light-stripers on Rocky and its derivatives (Volpe 1996), use the scanner data to recognize the presence of a discrete, positive obstacle. Our approach is similar in detecting steps, but differs in also detecting ditch and belly hazards. In general, we are not aware of any laser-based natural terrain hazard detector with equal or better performance in terms of miss rate (zero) and cycle time (better than 4 Hz).

2.1 Laser Rangefinder

The sensor of the laser system is an Acuity 3000-LIR laser ranger operating in the near-infrared band (Acuity 1993). It sends a beam towards a rotating mirror that projects a laser plane towards the ground at approximately 45 degrees. In the current configuration, the laser illuminates the ground 100 cm in front of the vehicle, which gives a 3D resolution under 1 cm. The effective field of view is limited by the effective angle of incidence, and is in practice 90 degrees. The rates at which data is available depends on the desired resolution, the number of samples per scan, and the maximum range detectable. In the run-time system, data is available approximately every 25-50 ms.

Correct estimation of the range requires that enough light be reflected back to the detector. In the general case, this requires that the illuminated surface be diffusely reflective. If the reflection is specular, the reading is corrupted by high variance and possibly a range offset. If the surface is not reflective but absorptive, as in the case of asphalt, then the weak return signal may cause detection to fail (no reading) or to return noisy measurements (spurious readings).

2.2 Hazard Detection

The on-board computer retrieves the range and angle data and performs a test to determine their validity. The data is then linearized and transformed into 3D coordinates in the local body coordinate system and this profile is processed to find evidence of the presence of terrain features hazardous to the vehicle. If such hazards occur or the frequency of scans with too much unreliable information is too high, an emergency stop signal is sent to the vehicle.

The system developed is a baseline ccnfiguration needing no dead reckoning data or any information about the plan of traverse. This means less processing leading to faster update rate and to independence from different vehicle systems. Even during total breakdown **of** the navigational computers and sensors the vehicle can still be controlled in safe teleoperation. The configuration is more conservative due to the limited amount of information used but sufficient in very hostile terrain.

2.3 Data Acquisition

The first step in processing a laser scan is to determine the integrity of the laser system and to perform self-diagnostics if necessary. The next step is to remove invalid data and to determine if the spatial density of the remaining data is high enough to reliably calculate the hazard rnetrics.

These calculations use a number of laser ranger sensor signals: Absolute encoder, incremental encoder, range, temperature, data out of range, buffer overflow, intensity of reflected light and ambient light. First the motor subsystem is checked through a test of correct motion of the mirror. This is done using three measures:

- **Is** zero pulse captured (absolute encoder)?
- Full cycle loaded? **+/- 45** degrees in front of the vehicle captured.
- **Is** motor spinning (incremental encoder)?

The zero pulse of the absolute encoder synchronizes the angles captured by the incremental encoder. If this pulse **is** missed, the absolute orientation of the sweep is unknown and the data is of no value. Both the capture and the synchronizing pulse and a successful acquisition of a full cycle depends on the motion of the mirror. If the mirror is spinning too fast the zero pulse may be missed and if spinning too slowly a full range may not be available within the number of samples recorded. As the mirror has relatively slow dynamics the system is designed so that the zero pulse or full angle measures have to fire a certain number of times before the spinning of the motor is tested. This avoids erroneous fault detection during start-up and temporary disturbances.

In addition to determining whether the mirror is spinning correctly a check is made of the laser temperature and whether there are internal errors (for example, buffer overflow) on the **SCSI** interface board, which indicate that samples have been lost. Finally the system assesses whether the density of reliable data is sufficient. A common problem is that the laser beam hits a terrain point which does not reflect enough light to make an accurate range estimation. This can be due to the angle of incidence, non-diffuse reflection, or a low reflectance of the object being measured (dark surface). This results in an unreliable datum, which can confound subsequent processing. **A** dependable way to detect zones of unreliable data is high variance between adjacent range readings or unlikely change in the average elevation of consecutive scans.

All checks, except for the variance in range estimates and unlikely change in average elevation, are very fast as their input are direct sensor signals, which are more or less dedicated for integrity analysis purposes. Only the high-variance and the unlikely average change test needs a non-trivial amount of computation to determine status. In any event, data acquisition **is** fast: including integrity checking and data testing, it can be done in about 180 ms (including *35* ms for the laser to generate range data).

When a problem occurs, corrective action is necessary. For some of the very low level problems, like mirror motion, appropriate actions can be directly associated with the problem. In the case of mirror motion problems, new scans are commanded to see if the problem was just a result of spurious unfavorable conditions. For other problems, such as high temperature, different actions can be taken involving other systems of the rover (like applying extra cooling, shutdown or seeking shade). Since other subsystems may also be affected by these kind of problems, in most cases the laser subsystem will just discard the data as invalid, and leave it to other systems to correct the problem.

The detection of a problem by the data acquisition metric signals an acquisition hazard indicating that no information **is** available. Otherwise when no metrics fire the valid data of the range scan is processed by the hazard metrics.

2.4 Hazard Metrics

Since the laser line hits the ground fairly close to the vehicle (approximately 100 cm in front of it). detection must be made quickly in order to react in time. For this reason, we have chosen to define simple heuristic rnetrics for each type of hazard that we want the laser to detect. These metrics are defined in terms of a single scan of the proximity sensor, so that no information needs to be saved between scans. Also

Type	Danger
Positive elevation (step)	Small, medium, large rocks
	Step (e.g., broken surface)
	Boulders
Negative elevation (ditch)	Ditch
	Step in landscape
	Craters
Cross slopes	Dunes

Figure 3. Terrain types

no information about the planned path of the rover is utilized nor is any dead-reckoning data used.

When designing the metrics two approaches were considered. One approach evaluates whether the elevation of the surface in front of the rover (represented in the rover's local coordinate frame) exceeds the capability of the rover. While this approach is fairly general and computationally very simple, it has the problem that the apparent elevation of the terrain in front of the rover is a function of both the actual terrain height and the rover's current inclination (e.g., if the front wheels of the rover are on small rocks, the elevation of the terrain one meter in front of the rover appears lower than it actually is). Thus, while true hazards will be detected reliably and quickly, there are situations where potential hazards will be detected erroneously, and the vehicle will be stopped unnecessarily.

The other approach involves identifying signatures of different landscape formations that are invariant to the motions that occur when driving over minor obstacles. For example, when obliquely approaching a downward slope, the range measurements will gradually increase starting at the point where the laser line intersects the beginning of the slope, forming an 'elbow bend'. This characteristic shape is evident regardless of whether the front of the rover is elevated by a rock, and so is less likely to detect hazards erroneously. However, in the signature approach it is difficult to quantify the danger a profile constitutes to the vehicle. For example, when approaching a minor downwards slope from different angles, the shift in range varies and so the steepness of the slope cannot be known. Thus, it is difficult to quantify what constitutes a real hazard. In addition, in the signature approach much more processing has to be performed, as the number of possible landscape feature signatures is relatively large compared to the number of rover limitations (Figure 3).

Another problem with the interpretation approach is that the set of features may not cover all possible landscapes encountered. Hence, safe operation would not be guaranteed. To ensure safety (at the cost of sometimes stopping erroneously), it was decided to employ the direct method

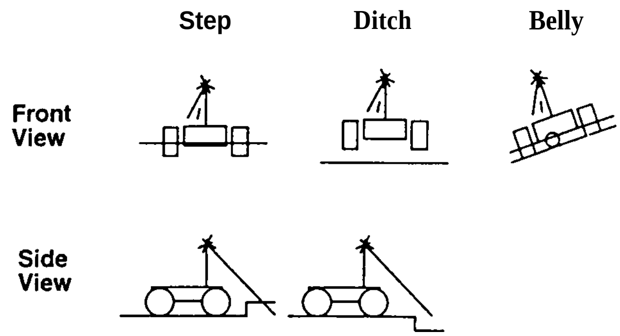

Figure 4. Physical metrics: Step, ditch, and belly hazards

based on the capabilities of the rover. Three hazard types are considered:

- Maximum traversable step (curb-like, head on)
- Maximum traversable ditch (curb-like. head on)
- Belly clearance

As the metrics are defined in terms of a single scan, no information is available about the transition from the surface currently under the rover to the scanned surface at the laser line. The transition must therefore be treated as a worst case, which is a step-like transition at the laser line. Also, since the laser subsystem does not know the current vehicle steer angle, to be safe it must analyze the complete laser line. For the step and ditch metrics, this translates into defining a simple upper and lower threshold (respectively) directly on the 3D elevation profile (Figures 3 and 4). The thresholds data is spatially filtered to prevent spurious signals from firing the metrics. A median filtering is used, which is quite fast since it operates in the binary domain (equation 1 for the step metric).

$$step = \left(\sum_{N=1}^{N_{max}-n_f} \left(\left(\sum_{n=1}^{n_f} (z(N+n) > z_{max}) \right) > \frac{n_f}{2} \right) \right) > W_{max} \quad (1)$$

where z is the elevation, z_{max} is step elevation threshold, n_f, is spatial filter length and W_{max} is the width threshold of the step hazard. N_{max} is the total number of samples in a scan line and the '>' operator is interpreted as yielding 0 if false, 1 otherwise.

The belly hazard metric first estimates the slope by linear regression and then equalizes the elevation profile accordingly, yielding a level elevation profile centered around zero elevation. Based on the minimum and maximum elevation in this compensated profile, the most favorable levels of a positive Z_{cmax} and a negative threshold Z_{cmin} is computed (difference between the two levels is the body clearance minus a margin. see equation 2).

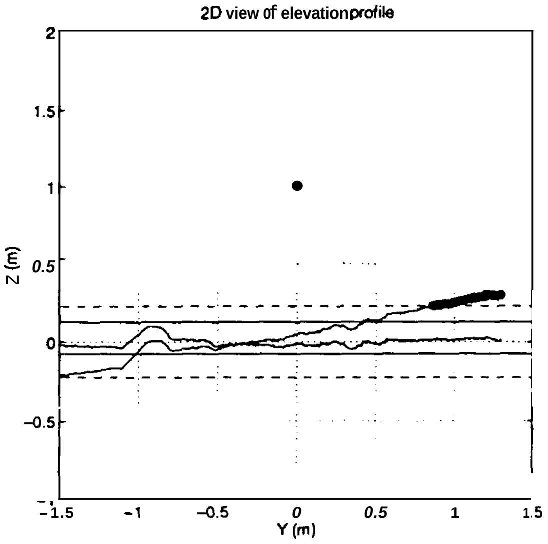

Figure 5. Hazard detection. The elevation profile is seen in the direc tion of travel from the vehicle. The laser is positioned at y=0, z=1.

$$\begin{bmatrix} Z_{cmax} \\ Z_{cmin} \end{bmatrix} = \frac{Z_{scancmax} - Z_{scancmin}}{2} + \begin{bmatrix} 1 \\ -1 \end{bmatrix} \frac{belly\ clearance}{2} \quad (2)$$

where $Z_{scancmax}$ and $Z_{scancmin}$ are the maximum and minimum elevation in the compensated elevation profile. The compensated elevation profile is then tested for exceeding the elevation band defined by the two threshold levels and this output is filtered spatially as for the step and ditch metrics. Since this metric is more computationally expensive than the other two, it is processed last (and only if the other two do not fire). The belly hazard metric is itself not capable of determining whether it is safe to enter the cross slope itself but only if there is a hazardous object on the slope.

As an example, Figure 5 illustrates the interpretation of a typical scene. The elevation profile is inclined to the left, relatively flat, and shows a small mound at y=-lm. The two dashed lines indicate the step and ditch thresholds. For y>0.5 the step metric has detected a hazard (denoted by 'o's). No belly hazard is detected as the compensated profile lies within the two solid belly thresholds.

2.5 Combining Acquisition and Physical Hazards

To reach the single stop/release signal accepted by the vehicle the output of the physical and acquisition metrics must be combined. A simple solution is to add the signal producing a logical **or.** In this configuration acquisition metrics and physical metrics are assigned equal weight or importance to the safety of the vehicle. However it is intuitively clear that a metric fired in the physical hazards group is more urgent or important to react on than a signal from an acquisition metric which essentially means that reliable data cannot be obtained. The acquisition metrics indicate that an obstacle ***may*** be covered by the laser scanner. The approach used therefore assigns less importance to the acquisition metrics than to the physical which positively reflects the presence of a hazard.

The inputs from the two groups are fed into a number of temporal filters each designed to react to a certain combination or occurrence of physical and acquisition hazards. One filter will react if 2 out of **3** scans show physical hazards indicating clear presence of a hazard. Another filter will signal if **4** out of 7 scans show acquisition hazards reflecting that it is unsafe to continue driving in an almost-blind manner. Yet other filters will fire if a physical hazard appears in conjunction with a number of acquisition hazards under the assumption that it is likely that the acquisition hazards in this case cover over a real physical hazard but that data was too unreliable to apply the physical metrics.

These filters are implemented as rank filters yielding a good suppression of spurious signals minimizing unnecessary stops. As the filters are of different length the response time is different having the shortest response for an obvious physical hazard. This small lag of q scans is taken into account when calculating the pose of the scanner to yield the needed look-ahead:

$$look\ ahead = ((q+1)t_{proc} + qt_{scan})v_{max} + d_{stop} \quad (3)$$

Under near-perfect conditions the fusion of acquisition and physical metrics will converge to the situation where the two groups are assigned equal weight as the number of acquisition hazards will decrease towards zero.

2.6 Performance

The integrity checks and hazard detection metrics have been implemented and tested in experiments on the Ratler vehicle to characterize their performance. The tests were conducted at a two-acre natural terrain site in Pittsburgh called the Moonyard, which was designed to replicate crater patterns and terrain features of the Apollo 11, Apollo 17, and Mare Tranquilitatis regions on the Moon.

In terms of missed hazards, the performance is excellent. In a large number of runs on a variety of lunar-like natural terrain such as craters. **rocks,** pits, slopes, and waves, the system missed ***no*** hazards at all and the vehicle was stopped consistently and reliably at a safe distance before the hazard. For a few terrain types such as rough terrain the stop was issued late, but the vehicle was still stopped at safe distance. Craters will generally be climbed up on the small rim and then the vehicle will stop at a safe distance to the crater itself. The algorithm does not detect slopes unless they are very steep and there is an abrupt change between the flat ground and the slope. However the slope or the transition to the slope does not constitute a hazard to the vehicle in the sense that it can get stuck or hit some terrain feature. It is up to other systems to incorporate inclination aspects into the safety measures.

Few false detections are encountered, mainly due to specular reflecting surfaces and small angles of incidence. This is, however, very dependent on the scene used for testing and the pose of the laser scanner. Some of these problems can thus be overcome by placing the sensor in a more favorable location. These kinds of unnecessary stops are intermittent and are self-correcting in 0.5-1 second. Another kind of unnecessary stops are encountered when climbing waves or undulations of long spatial period (in order of several meters). As the laser range is converted into an elevation with respect to the vehicle body the laser system will encounter a drop when climbing a wave as the laser hits a point on the other side of the wave. Similarly when descending on a wave the start of another wave will cause a step metric to stop the vehicle. This is inherent to the stand-alone configuration as the system cannot resolve this slow or a more hazardous transition using only one laser scan.

The cycle time is currently about 4 Hz on a 66 MHz 486 in the test configuration. This includes no effort for optimizing the algorithms, relatively dense sampling, and a high range precision, which requires more time by the laser (currently 15% of the total time). It is expected that the speed can be increased considerably without significant loss of detection reliability by streamlining code and reducing range precision to more realistic values. For most of the tests a speed of 0.14 m/s was used. However speeds up to 0.4 m/s have been tried showing satisfactory performance, that is, no hazards missed. In all, the laser proximity safeguarding has proven to be a very valuable supplement to the overall navigation system.

3 Safeguarded Teleoperation Field Trials

We tested the safeguarded teleoperation system at three different sites: the Moonyard, the Highbay, and the Slagheap.

The Moonyard (Figure 6) is an artificial lunar analogue site occupying 2.5 acres and featuring 12 craters. This site contains terrain patterned after three distinct lunar areas. The Apollo 17 analogue features scaled models of the Shakespeare, Camelot, Victory, Bronte, and Shorty craters, located between models of the North and South Massifs. The **Apollo** 11 analogue contains a model of West Crater with its two distinctive "ears". The Mare Tranquilitatis analogue contains flat, cratered terrain. Throughout the site, the crater depth is half the diameter, following the proportions of the smaller lunar craters. The largest crater measures over 14 meters in diameter.

Figure 6. Ratler traversing the Moonyard

The Highbay is an indoor facility with a concrete floor. We performed testing here during inclement weather. Obstacles in this test area included robots, I-beams, furniture, trucks, forklifts, equipment racks, railing, barrels, posts, and boxes.

The Slagheap is a IO-acre slag dump with little vegetation. We conducted testing here for two principal reasons. First, the site afforded different terrain types, and so allowed us to verify that we were not unconsciously "tuning" the safeguarding system to work particularly well at the Moonyard. Second, the terrain dried significantly faster than did the terrain at the Moonyard, and so enabled additional outdoor testing.

The safeguarded teleoperation trials proceeded by setting the Arbiter control mode from 'User is Boss' to 'User is Partner'. In this mode, the user and safeguarding system both cast votes for driving velocities, and the Arbiter arbitrates these votes and sends speed and steering commands to the vehicle controller.

In practice, the user tended to cast votes only under certain conditions:

- To halt the vehicle for safety reasons. We call such a halt an ***intervention.***
- To halt the vehicle for logistics reasons such as swapping out batteries, taking shelter from rainstorms, and repairing components.
- To exercise the safeguarding system, for example, intentionally steering **at** a discrete obstacle.
- To save time at the boundary. Under autonomous control, the rover (correctly) halts at the boundary of the test area, and then begins a recovery procedure, which may include backing up, turning a modest amount (less than 10 degrees), and turning a significant amount (several tens of degrees). Depending on the terrain, this recovery procedure can take up to

Test Site	Obstacle Density	Distance Traversed (km)
Moonyard	Higher	13.3
Highbay	Medium	17.4
Slagheap	Lower	12.0
Combined	—	42.7

Module	N	Time (ms)
Laser	—	250
Stereo	79	1,822
Planning	480	1,645

Figure 8. Median cycle times over N cycles

several minutes to complete. To avoid this wait, users tended to steer away from the boundary.

Trials were conducted under a wide variety of conditions ranging in lighting from dawn to dusk, in weather from rain to shine, in wind from still to violent, and in ground moisture from baked dry to deep puddles.

The test procedure required at least two people: the driver seated at a workstation in a truck parked outside the test area; the safety officer within view of the robot, and in dangerous terrain, within reach of the rover's kill switch.

A majority (perhaps 70 percent) of the driving was performed by one user, and a minority (perhaps 20 percent) was performed by two other individuals, and a small fraction (perhaps 10 percent) was performed by a half-dozen other users, some novices and some veterans.

Testing required approximately one hour of setup and one hour of teardown. The bulk of this time was dedicated to antenna mounting and cabling.

4 Field Trial Results

We conducted field trials during the summer of 1996. Figure 7 tabulates the distance traversed at each of the three sites, totalling almost 43 km. The typical travel speed under safeguarded teleoperation control was 50 cm/sec, although the rover successfully travelled at its maximum speed of 70 cm/sec while safeguarding.

Figure 8 tabulates the median cycle times for the three primary safeguarding modules. The stereo and planning modules executed on the same Pentium **133** running the Linux operating system. Note that their cycle times are measured by operating system calls during operation of the safeguarding system, and as a consequence the times include delays due to interprocess communications (including message blocking), disk i/o, memory swapping, network collisions, network dropouts, and PCI bus i/o related to image digitization. For the stereo timing, the processing included image and pose acquisition, image rectification, normalized correlation, and conversion to Cartesian coordinates. The stereo algorithm computed 156 disparities and performed correlation in a 25x17 window. The distribution of times had a standard deviation of 107 ms. For the planning timing, the algorithm processed an average of 4,342 elevation points per cycle, with a typical lookahead distance of 4 to 8 meters, a typical ground resolution of 8 cm, and a total **of** [illegible] arcs evaluated per cycle. The distribution of times had a standard deviation of 49 ms. Note that the processing for stereo and planning is interleaved.

During the field trials, the driver noted each and every occasion at which the safeguarded system did not adequately protect the rover from danger. Examples of failure include colliding with a rock (which occurred several times), tipping over (which never occurred). We observed 2.4 failures **per** kilometer (16 failures over 6.7 km) using stereo-based safeguarding alone, and 0.8 failures per kilometer (36 failures over 42.7 kmj using multi-sensor safeguarding with stereo and laser. This indicates that the multi-sensor approach is **3** times more effective than the stereo-based approach.

Previous versions of the safeguarding system crashed every kilometer or so due to memory exhaustion. This version ran indefinitely, exhibiting almost no memory leaks.

5 Discussion

This paper described the addition of a laser sensing system to an existing system for safeguarded teleoperation of a remote rover. The paper presented the results of an extensive and realistic testing program that demonstrate conclusively that the multi-sensor system is more effective and more reliable than the previous single-sensor system.

Although the implemented laser system proved effective, numerous improvements are possible. One major extension would incorporate information about vehicle movements and also use previous scans. This will enable the laser system to maintain a representation of the terrain in front of the rover, enabling more sophisticated three-dimensional hazard analysis to determine, for example, whether the vehicle is about to enter a slope which is too steep. This extension would bring the **work** close to the work by **(Krotkov** 1994) but without the 2D scanner.

Like the laser system, the overall multi-sensor safeguarding system proved effective, but affords numerous opportunities for improvement. First, turning maneuvers after the laser system has detected an obstacle should be

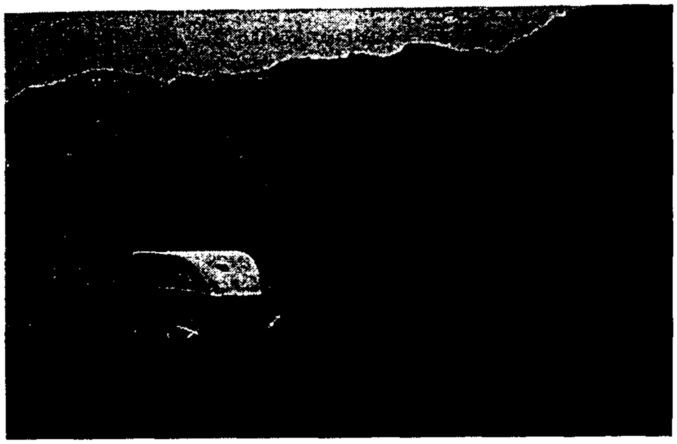

Figure 9. Nomad

executed at lower speed. This will mitigate the effect of unforeseen collisions during the rotation. Second, the stereo cameras should cover a wider field of view than 80 degrees. This will improve the rover's ability to maneuver around obstacles.

Future work will port the multi-sensor safeguarded teleoperation system to a new vehicle (Figure **9)** and demonstrate a 200 km traverse over the Atacama desert in Chile during the Summer of 1997.

Acknowledgments

We gratefully acknowledge the assistance of Lonnie Chrisman, Cassandra Coombs, Fabio Cozman, Keith Duwel, David Pahnos, James Martin. Patrick Muir, Mesta Electronics, Jay Tuchinda, Greg Whelan, and Red Whittaker. This work was supported in **part** by NASA Grants NAGW-I 175 and NAGW-*3863* from the NASA Telerobotics Program.

References

R. Chatila, S. Lacroix, S. Betge-Brezetz, M. Devy, T. Simeon. Autonomous Mobile Robot Navigation for Planet Exploration: The EDEN Project. In Proc. Workshop on Planetary Rover Technology and Systems, IEEE Intl. Conf. Robotics and Automation, April 1996.

L. Henriksen. Laser Ranger-Based Hazard Detection. Technical Report CMU-RI-TR-96-32, Carnegie Mellon University. August 1996.

A. Kelly. Concept Design of a Scanning Laser Rangefinder for Autonomous Vehicles. Technical Report CMU-RI-TR-94-21, Carnegie Mellon University, 1994.

E. Krotkov and R. Hoffman. Terrain Mapping for a Walking Planetary Rover. *IEEE Trans. Robotics and Automation,* vol. 10, no. 6, December 1994.

E. Krotkov, M. Hebert, and R. Simmons. Stereo Perception and Dead Reckoning for a Prototype Lunar Rover. *Autonomous Robots*, 2(4):313-331, December 1995.

E. Krotkov. J. Bares. L. Katragadda. R. Simmons and R. Whittaker. Lunar Rover Demonstrations with Dante and Ratler. In Proc. Intl. Symposium on Artificial Intelligence, Robotics and Automation for Space. JPL, Pasadena, CA, October 1994.

J. Purvis and P. Klarer. RATLER: Robotic All Terrain Lunar Exploration Rover. In Proc. Sixth Annual Space Operations, Applications and Research Symposium. Johnson Space Center, Houston, 1992.

Acuity Research. Accurange 3000-LV and Accurange 3000-LIR Users's Manual. Rev 1.1 August, 1993.

R. Simmons, E. Krotkov, L. Chrisman, F. Cozman, R. Goodwin, M. Hebert, G. Heredia, S. Koenig. P. Muir, Y. Shinoda and W. Whittaker. Mixed-Mode Control of Navigation for a Lunar Rover. In Proc. SSI Space Manufacturing Conf., Princeton. New Jersey, May 1995.

R. Simmons, L. Henriksen, L. Chrisman and G. Whelan. Obstacle Avoidance and Safeguarding for a Lunar Rover. In Proc. AIAA Forum on Advanced Developments in Space Robotics, Madison. Wisconsin, August 1996.

R. Volpe, J. Balaram. T. Ohm. R. Ivlev. The Rocky 7 Mars Rover Prototype. In Proc. Workshop on Planetary Rover Technology and Systems, IEEE Intl. Conf. Robotics and Automation, April 1996.